

# Crustal melting by ponding of mafic magmas: A numerical model

Norbert Laube<sup>\*</sup>, Jörn Springer

*GeoForschungsZentrum (GFZ), Telegrafenberg, Haus G, D-14473 Potsdam, Germany*

Received 23 July 1997; accepted 30 October 1997

## Abstract

We examine the possibility that an abating period of mantle-related volcanic activity at continental margins triggers the production of crustal-derived melts. A vertical zone, permeated by rising mafic melts, is established below the volcanic arc if long-lasting mantle-derived magmatism occurs. This situation can be assumed to exist at continental arcs. We propose that mafic magmas release heat and water into the crustal environment, if subsequent magma ascent is stopped due to establishment of a density barrier. This process enhances intracrustal partial melting. Using a finite-element program, we simulate in a 2D model area the time-dependent change of the crustal thermal structure. The spatial distribution of potential melting zones and their degree of partial melting within the crust is computed. The amount of generated melt able to segregate is calculated and compared with volume estimates given by field investigation and geochemical constraints in a natural test case. We chose the Altiplano–Puna volcanic complex (APVC) which is part of the central Andes, as an example where the process may have happened and show, from simple approximations, that the model can explain the volumes of crustal melts represented by the felsic volcanics in this region. Although the model parameters and assumptions used are specific to this geologic context, the proposed model is generally applicable to any arc setting. © 1998 Elsevier Science B.V.

*Keywords:* crustal melting; mafic magma; numerical modelling; ponding

## 1. Introduction

Magmatic activity at active continental margins is characterized by the occurrence of both primarily mantle-derived basic to intermediate melts of basaltic to andesitic compositions, and felsic melts of dacitic to rhyolitic compositions (e.g. Crisp, 1984). The volumetric ratios between mafic and felsic volcanics vary with time and space along the extension of the volcanic arc.

Trace-element and REE patterns of the mafic magmas in continental arcs give evidence for various degrees of crustal influence; isotope data indicate

that the felsic volcanics are primarily crustal-derived (Schmitt-Riegraf and Pichler, 1988; Asmerom et al., 1991; Coira et al., 1993; Francis and Hawkesworth, 1994; Graham et al., 1995).

If the felsic volcanics are crustal melts, what caused this melting?

Hochstein (1995) discussed plastic deformation processes within the ductile lithosphere as a heat source to explain endogenous crustal heating in the northern part of the Tonga–Kermadec arc system. Zen (1988, 1992) shows that, within a tectonic setting of a overthickened crust (e.g. central Andes), intracrustal melting may be a consequence of multiple thrusting of upper crustal material alone, without the requirement of external heat transfer. Zen (1988) and Sandiford and Powell (1990) predict that thrust-

<sup>\*</sup> Corresponding author. Tel.: +49-331-2881345; fax: +49-331-2881328; e-mail: laube@gfz-potsdam.de

ing alone leads to a time lag of some 10 Ma before large-scale crustal anatexis begins.

Another mechanism which relates a thick crust to

enhanced crustal anatexis in a continental arc setting may result from the fact that mafic magmas either have to rise through greater distances before erup-

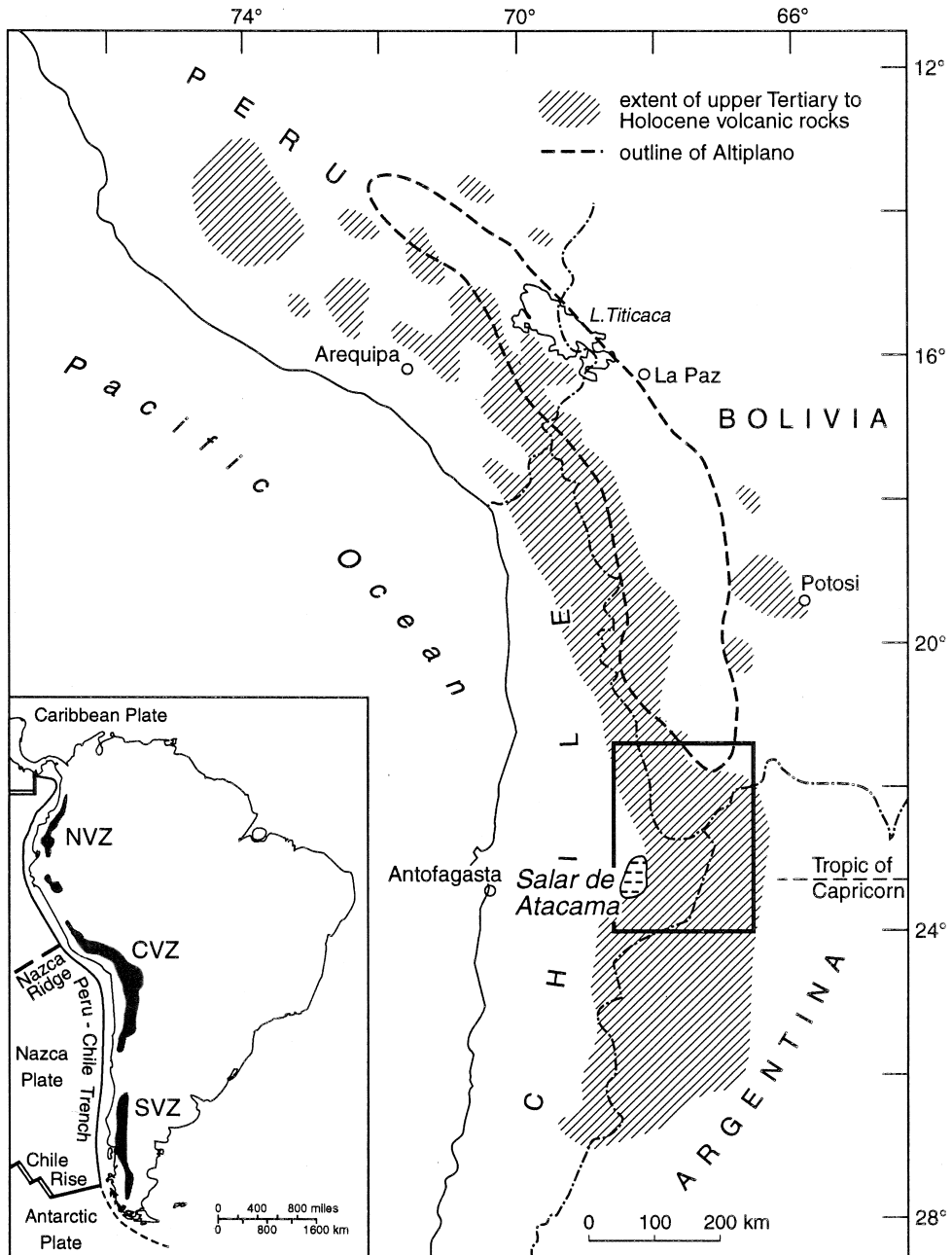


Fig. 1. Sketch map of locations (slightly modified after DeSilva (1989a) DeSilva (1989b)). The solid rectangle outlines the Altiplano-Puna volcanic complex. Inset map shows the volcanically active segments of the Andes separated by volcanic gaps. NVZ: northern volcanic zone, CVZ: central volcanic zone, SVZ: southern volcanic zone.

tion, or they became buoyantly ponded at the crust–mantle boundary or within the crust. In both cases, the opportunity for physical and chemical magma–crust interaction generally increases (e.g. Leeman, 1983; Tepper et al., 1993). Part of this interaction is thermal since the mafic magmas introduce heat into the crust, causing intracrustal melt generation. The general principles of this melt-forming process have been discussed extensively by a number of authors (e.g. Patchett, 1980; Huppert and Sparks, 1988a,b; Marsh, 1989; Bergantz and Dawes, 1994).

In this paper, we explore the idea that abating mafic volcanic activity at a continental margin may trigger crustal melting when the channelized flow of mafic magma is arrested and the mafic conduits thermally equilibrate with their crustal environment. Water released from the freezing mafic magma further enhances crustal partial melting.

For the basic data to generate a simplified model, we chose the Altiplano–Puna volcanic complex (APVC) of the central Andean volcanic zone (CVZ) (Fig. 1) as a prominent example of an active continental margin, where silicic melt abundance seems to coincide with a thickened crust, and the proposed mechanism may have happened. Here, the chemical nature of volcanic products changed with time. Since the last Miocene, the mean composition of andesitic magmas became more evolved, and the degree of crustal contamination increased. The more dramatic change was the comparatively sudden appearance of rhyodacitic and dacitic ignimbrites, whose abundance rose sharply in the Late Tertiary, and decreased again in the Quaternary. During the ‘ignimbritic stage’, the extent of mafic volcanism diminished.

Using a finite-element program, we simulate the time-dependent change of the crustal thermal structure in a 2D model area as a result of thermal break-down of a mafic magma conduit zone. The temperature evolution in the upper lithosphere is coupled with phase stability derived information regarding phase boundaries and stability fields of different water-bearing minerals common in crustal rocks. Intracrustal melting is numerically simulated in dependency on temperature, pressure and water budget. The spatial distribution of melting zones and their degree of partial melting are computed. Taking into account various threshold values of partial melt-

ing necessary for melt to escape, the amount of potentially segregable melt is calculated and compared with volume estimates provided by field investigation and geochemical constraints. The calculated depths of crustal melt formation (e.g. at the base of crust or within the crust) help constrain whether underplating or melt ponding at higher levels caused the melting process.

Our model places limits on crustal melt volumes which can be produced by the proposed mechanism. A detailed model of the geochemical evolution of both melts (mafic and felsic) can not be given, as the processes of assimilation, fractionation, and mixing occurring during heat and mass transfer between intruded melts and melting wall rock are too complex (e.g. Grove et al., 1988).

## 2. Background

This chapter gives some basic background for the numerical model. The notation used is given in Table 1.

### 2.1. Estimation of the water budget

The amount of water available in the potential crustal source region controls the extent of partial melting and the chemical composition of the generated melt (Tepper et al., 1993).

In our model, the extent of melting processes is governed by the water content of the source rock. CO<sub>2</sub> is assumed to be an inert component at crustal pressures (< 1.5 GPa), which only slightly increases the liquidus temperatures by lowering the H<sub>2</sub>O-fugacity. Other volatiles as H, Cl, F are not considered.

The total water content  $C^r$  in wt% of the source rock is the sum of a number of sources. In the model, three sources of water are taken into consideration:

- (1)  $C_0^r$  is water fixed by surface adsorption on mineral grains and capillary water.
- (2)  $C^{\text{reac}}$  is water released by OH-bearing mineral phases.
- (3)  $C^m$  is water released into country rock by crystallisation of mafic magmas.

Thus,  $C^r = C_0^r + C^{\text{reac}} + C^m$ . The estimation of the single variables is described in the following sections.

Table 1  
Initial values and other parameters used

	Symbol	Value	Unit	Meaning
Mafic melt	$T_s^m$	1075	(°C)	solidus temperature
	$T_l^m$	1175	(°C)	liquidus temperature
	$L^m$	$4 \times 10^5$	(J kg <sup>-1</sup> )	latent heat of crystallisation
	$c^m$	1480	(J kg <sup>-1</sup> )	melt heat capacity
	$\Phi$	0.2		initial volume fraction within conduit zone
	$s^m$			H <sub>2</sub> O saturation level
	$C_0^m$		(wt%)	H <sub>2</sub> O content in saturated melt
	$C^m = \Phi \cdot s^m \cdot C_0^m$		(wt%)	H <sub>2</sub> O released by crystallizing melt
	$X^m$			melting degree
	$\rho^m$	2.80	(g cm <sup>-3</sup> )	melt density
Silicic melt	$s^s$			H <sub>2</sub> O saturation level
	$C_0^s$		(wt%)	H <sub>2</sub> O in saturated melt
	$C^s = s^s \cdot C_0^s$		(wt%)	H <sub>2</sub> O content
	$\rho^s$	2.65	(g cm <sup>-3</sup> )	melt density
Crust	$T_s^r$		(°C)	solidus temperature
	$T_l^r$		(°C)	liquidus temperature
	$T$		(°C)	temperature
	$L^f$	$3 \times 10^5$	(J kg <sup>-1</sup> )	latent heat of fusion
	$c^r$	1000	(J kg <sup>-1</sup> )	rock heat capacity
	$C_0^r$	3.0	(wt%)	initial crustal H <sub>2</sub> O content
	$C^{\text{reac}}$	≤ 1	(wt%)	H <sub>2</sub> O derived from mineral decomposition
	$C^r = C_0^r + C^{\text{reac}} + C^m$		(wt%)	total crustal H <sub>2</sub> O content
	$f$			melting degree derived from $C^r$
	$F$			melting degree derived from $T$
	$X^r = \min(f, F)$			melting degree
	$\rho^r$		(g cm <sup>-3</sup> )	density

$L^m$ : Turcotte and Schubert (1982);  $c^m$ : Rivers and Carmichael (1987);  $L^f$ : Huppert and Sparks (1988a,b);  $c^r$ : Singer et al. (1989).

### 2.1.1. The basic crustal water content

Within the middle and lower crust, gneissic rocks of amphibolite metamorphic grade and acid or mafic granulites dominate the lithology. We assume a constant value of 3.0 wt% for the average initial crustal water-content  $C_0^r$  (for further explanation see Section 3.2).

### 2.1.2. Mineral dehydration reactions

The most common lithologies of the crust contain < 30% hydroxyl-bearing minerals (sum of micas and amphiboles). Assuming a modal relation of 1:1:1 between muscovite, biotite and amphibole the water contributed by mineral dehydration reactions amounts to only ≈ 1.0 wt%, if the water contents of these minerals are assumed to be 4, 4, and 2 wt% per formula unit, respectively. Thus, for calculation, we increase  $C^r$  in each case by 0.4 wt% if muscovite and biotite break down, and by 0.2 wt% if horn-

blende decomposes, so that  $C^{\text{reac}} \leq 1$  wt%. The liberated water is directly transferred to the melt. For the model we use the following dehydration reactions (Whitney, 1988; Philpotts, 1990):

- muscovite (out):  
musc + qz + Na-fsp ↔ sill + K-fsp + melt,
- biotite (out):  
bio + qz + Na-fsp ↔ K-fsp + pyx + melt,
- hornblende (out):  
hbl + qz + fsp ↔ pyx + melt.

The equations for the numerical description of the petrogenetic grid are listed in the Appendix A. Fig. 2 shows the  $p$  and  $T$  dependence of the reactions. Other water-bearing mineral phases as chlorite, staurolite, cordierite or epidote are neglected.

### 2.1.3. Water contents of mafic and felsic magmas

Our estimate of the maximum amount of water contributed by the crystallization of mafic magma is

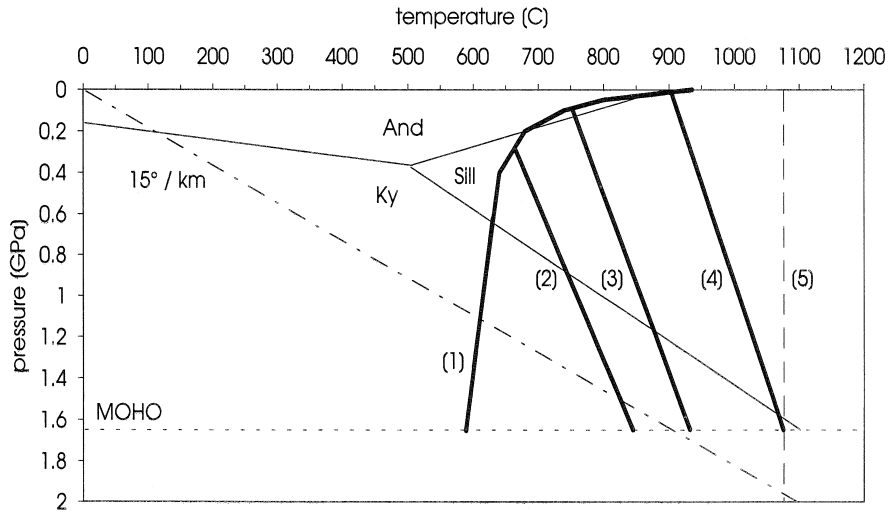


Fig. 2. Simplified petrogenetic grid used for model calculations within the crust. For orientation, a linear temperature gradient (– · –) of 15°C km<sup>-1</sup> is given, whereby 0.0275 GPa km<sup>-1</sup> are assumed. Numbers indicate the following reactions (Whitney, 1988; Philpotts, 1990): (1) water saturated solidus for granitic composition, (2) musc + qz + Na-fsp ↔ sill + K-fsp + melt, (3) bio + qz + Na-fsp ↔ K-fsp + pyx + melt, (4) hbl + qz + fsp ↔ pyx + melt. All reaction lines for  $p_{\text{lith}} = p_{\text{H}_2\text{O}}$ . At  $p_{\text{lith}} < 0.6$  GPa, the melt generating reactions (2–4) may change to vapor generating reactions (L → vapor). (5) shows the solidus temperature of andesite. The stability fields of the Al<sub>2</sub>SiO<sub>5</sub> polymorphs are from Holdaway (1971) (thin solid lines).

based on the investigations of water solubility in melts by e.g. Burnham (1975), Mysen (1977) and Holtz et al. (1995). This work has shown that the solubility is mainly a function of pressure. Only a small dependence on magma temperature has been demonstrated. Neglecting minor compositional effects, the maximum water contents  $C_0^m$  and  $C_0^s$  (wt%) of basaltic and intermediate-silicic melts at a given pressure (GPa) are approximated by the following Eqs. (1) and (2), which are based on the data given by Burnham (1975):

$$C_0^m = \sqrt{1.8935 + \frac{P}{0.00571}} - 1.38 \quad (1)$$

$$C_0^s = \sqrt{1.5898 + \frac{P}{0.00446}} - 1.26 \quad (2)$$

As basaltic magmas are commonly water undersaturated  $C_0^m$  is corrected by a factor  $s^m$  indicating the degree of saturation, with  $0 \leq s^m \leq 1$ . In a first approach we assume equal densities of mafic melt and wall rock. With  $\Phi$  as the mafic melt fraction within the conduit zone, the amount of water gained through mafic magma crystallisation is given by:

$$C^m = \Phi \cdot C_0^m \cdot s^m. \quad (3)$$

In the same manner, variations of the water saturation level within the generated silicic melt at the depth of origin are taken into account, introducing a factor  $0 \leq s^s \leq 1$ , so that:

$$C^s = C_0^s \cdot s^s. \quad (4)$$

### 2.2. Estimation of melt fraction within the country rock

It is well established that felsic magmas are commonly water-undersaturated and therefore, the melt volume is small at low temperatures. In dry systems, high degrees of melt can only be generated at high temperatures (Johannes and Holtz, 1991).

Water-saturated melting within the crust is the exception, although a granitic melt will absorb any available free water (e.g. Johannes and Holtz, 1990). Hyndman (1981) gives an overview of the influence of different mineral dehydration reactions on the source region and emplacement depths of granitic magmas.

Under water-undersaturated conditions (i.e. no excess water), and provided that water in the source rock is totally dissolved in the melt, an upper limit  $f$

of the degree of melting for water-saturated melt within a rock is given by:

$$f = \frac{C^r}{C^s}. \quad (5)$$

Alternatively we can estimate another upper limit  $F$  for the degree of crustal melting based on temperature, see Eq. (8) below. Using the digitized experimental data for the granitic system given by Johannes and Holtz (1991), we calculate the rock liquidus temperature  $T_1^r$  and the water-saturated solidus temperature  $T_s^r$  for any calculated crustal water content and pressure.

To find a minimum, we use the lower value,  $f$  or  $F$ , for further calculations:

$$X^r = \min(f, F). \quad (6)$$

### 2.3. The critical melt fraction required for melt segregation

The threshold value of the melt fraction  $X^r$  required for large-scale melt segregation within a crustal rock matrix is uncertain. Depending on a variety of parameters, values between 0.2 and 0.4 (e.g. Hyndman, 1981; Wickham, 1987), and values up to almost 0.5 (Arzi, 1978) have been discussed. Vigneresse et al. (1996) distinguish between a liquid percolation threshold (LPT) at  $X^r \approx 0.08$  and a melt escape threshold (MET) which is reached for dehydration melting conditions at  $X^r$  between 0.2 and 0.25, i.e. above 800°C. Van der Molen and Paterson (1979) estimated a critical melt fraction (CMF) of approximately 0.3 to 0.35 leading to a suspension-like behaviour of the partially molten bulk rock. This threshold value is expected to be irrespective of rock composition, deformation rate and mechanism of the solid rock matrix.

Von Bargen and Waff (1986) showed from geometrical considerations that  $X^r$ -values on the order of about 0.01 are necessary to ensure the interstitial connection of separate melt pockets. From numerical modeling Barboza and Bergantz (1996) estimated a 'low melt fraction window' in partially molten pelitic rock for  $0.05 < X^r < 0.15$ , which bars an accumulation of a substantial percentage of melt in the melting region. They postulated that melt existing in this range of melt fraction is most likely to be extracted.

For discussion, we chose 0.25 as the critical value in concurrence with Thompson and Connolly (1995) and Vigneresse et al. (1996); however, it must be considered, that the chemistry of the volcanic products will change depending on this assumption.

Partial melting characterized by  $X^r < 0.2$  is assumed only to cause migmatization although under certain circumstances migmatitic dikes could join to make larger magma bodies, finally able to rise through the crust.

### 2.4. Evolution of the thermal field

The temporal development of the thermal field during cooling of magma is described by the time-dependent heat balance equation:

$$c\rho \frac{\partial T}{\partial t} + \frac{\partial X^r}{\partial t} \rho^r L + \frac{\partial X^m}{\partial t} \rho^m L^m = \text{div } \lambda \text{ grad } T + A. \quad (7)$$

The last two terms on the left-hand side represent the latent heat associated with the change of the melting degrees  $X^r$  and  $X^m$  of the country rock and the mafic melt, respectively. These melting degrees are here assumed both to depend directly on temperature  $T$ :

$$X^i = \begin{cases} 0 & : T < T_s^i \\ \frac{T - T_s^i}{T_1^i - T_s^i} & : T_s^i \leq T \leq T_1^i \\ 1 & : T > T_1^i \end{cases} \quad (8)$$

where  $i$  is  $r$  or  $m$ , and  $T_1^i$  and  $T_s^i$  are the liquidus and solidus temperatures. As in our model, the liquidus temperatures are dependent on the water content (Fig. 2),  $X^r$  increases stepwise with  $T$  if decomposition reactions of water-bearing mineral phases occur. This discontinuous rock melting behaviour is shown for different lithologies by, e.g., Bergantz (1989) and Bergantz and Dawes (1994). The linear relation in Eq. (8) between melting degree, rock solidus and liquidus temperature, and ambient temperature is chosen as a simplification of the highly complex natural processes of heterogeneous rock melting.

The time-dependence of  $X^i$  is given by:

$$\frac{\partial X^i}{\partial t} = \frac{1}{T_1^i - T_s^i} \frac{\partial T}{\partial t}, \quad (9)$$

which allows us to replace the left side of Eq. (7) by  $C \cdot \partial T / \partial t$  with:

$$C = c\rho + \frac{\rho^r L^r}{T_1^r - T_s^r} + \frac{\rho^m L^m}{T_1^m - T_s^m} \quad (10)$$

for  $T_1^m \leq T \leq T_s^m$  (crystallisation interval).

Thompson and Connolly (1995) mentioned that endothermic and exothermic reactions due to metamorphic reactions have only a small effect on the general temperature field as their heat budgets are orders of magnitude smaller than the crustal radiogenic heat production. Thus, we neglect these effects for calculating the temperature field. Convective heat transport by fluids is not included since the movement of fluids in the deep lithosphere is only poorly understood. Barboza and Bergantz (1996) showed that the change from ‘conduction-dominated’ to ‘convection-dominated’ heat transfer by partial melt is strongly dependent on viscosity, time, and CMF. Convective flow sufficient to influence the thermal evolution does not occur until a critical melt fraction of  $\approx 0.35$  is exceeded. Since we focus our attention on the melt-forming process within the source region, no heat transfer due to advective melt transport is calculated.

### 3. The model scenario

#### 3.1. The model of lithospheric structure

The following 2D model is proposed as a simplification of a crustal section which may be considered as representative for the central part of the Andean

volcanic zone (modified after Schmitz, 1994): The lateral extension of the model box is 225 km. Given a subduction angle of  $25^\circ$  (e.g. Wilson, 1991), the slab reaches a depth of 80 km about 190 km from the trench. This point is the lower left corner of the model box. The volcanic arc is positioned in the middle of the box, 300 km behind the trench.

Structurally, the model lithosphere consists of three layers: (1) the upper crust; (2) the lower crust; and (3) the uppermost part of the lithospheric upper mantle.

As shown in Fig. 3, the supposed structure considers a continental crust of 60 km thickness, underlain by normal lithospheric mantle. The crust and the uppermost mantle are intersected by a vertical zone of 25 km width. Recent geophysical investigation gives evidence for such a zone, characterized by high electrical conductivity, strong negative Bouguer anomaly and high seismic attenuation (e.g. Schwarz et al., 1994; Schwarz, 1995; Schilling et al., 1995). This anomaly is assumed to be caused by the presence of melt. Alternative reasons fail to explain the extent of the anomaly as they require unrealistic high crustal amounts of either carbon or water.

We consider this zone to be the expression of a magma conduit zone and interpret the recent geophysical situation as representative for a long-standing mafic conduit zone in the Andean arc.

To define the initial situation for the numerical model, we extend this zone up to surface, although the geophysical anomaly is strongest at and below 20 km. The material in the model conduit zone is composed of a mixture of 20% mafic melt and 80% crustal rock at the initial stage (see Section 3.2). This

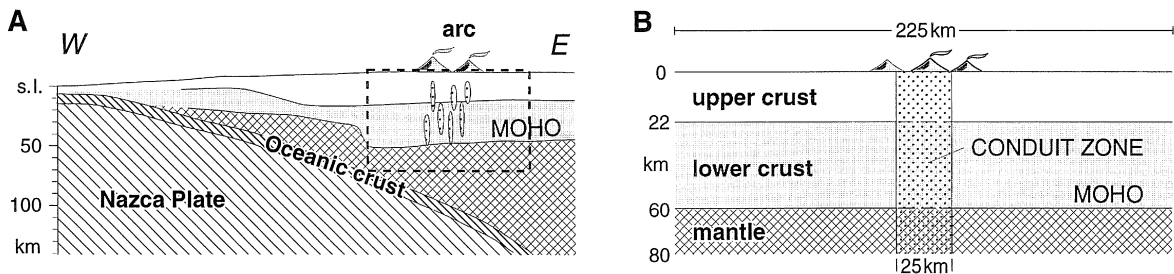


Fig. 3. (A) Interpretative E–W cross section of the Andean lithosphere at  $22^\circ\text{S}$  (modified after Schmitz, 1994). The small lenses below the volcanic arc suggest ascending mantle-derived melts. The dashed rectangle outlines the approximate position of the model area shown in (B). (B) model chosen for numerical simulation. For more details see text.

ratio fits the interpretation of the geophysical anomaly.

For each lithological unit, individual physical parameters are assigned. Table 2 gives the physical properties of the lithosphere model used for calculations. The data for the radiogenic heat production  $A$  and thermal conductivity  $\lambda$  are from Schatz and Simmons (1972). The temperature dependence of  $\lambda$  was neglected because the values range between 1.0 and 3.0 W m<sup>-1</sup> K<sup>-1</sup> within a temperature interval from 0° to 900°C for the most common crustal rocks (e.g. Touloukian et al., 1989; Arndt et al., 1995). The temperature dependence decreases with increasing temperature. Densities and depth intervals of lithosphere layers are according to Omarini and Götze (1991).

Besides the differential Eq. (7), initial and boundary conditions are needed. A temperature of 1200°C at a depth of 80 km is assumed according to Wyllie (1984) and Peacock (1993). This implies a warm mantle wedge which is heated by subduction-induced asthenospheric mantle flow, or corner flow (e.g. Tovish et al., 1978; Dvorkin et al., 1993). The undisturbed surface temperature is set at 0°C. At the left and right margins we assume zero horizontal heat flux as the usual boundary condition.

### 3.2. 4-stage model

The proposed model scenario is illustrated in Fig. 4.

**Stage 1, magma input from mantle:** Ongoing magma input from mantle through the crust results in mafic (andesitic) volcanism, focussed in a conduit zone under the active arc. This zone is both a physical and a chemical anomaly. As long as the pulsed withdrawal of andesitic magmas keeps pace with supply (steady state), the country rock temperature field remains little affected.

**Stage 2, evolution of a density barrier:** Increased magma input from the mantle due, e.g., to a change of subduction geometry (e.g. Pardo-Casas and Molnar, 1987) results in a further temperature rise within the crust and a partial melt zone (PMZ) forms. Assuming average densities (g cm<sup>-3</sup>) of: lower crust 2.83, crustal partial melt 2.65, mafic melt 2.80 (Table 2; Petford et al., 1993), the lower crust has to be molten to a degree of 17% to build up a density barrier for the ascending mantle-derived melts. Within this PMZ, processes as melting, assimilation, storage, and homogenisation (MASH) between mafic melts and induced crustal partial melts can occur (Hildreth and Moorbath, 1988).

The temperature of the mafic magma within the conduit zone during subsequent ascent is constrained as follows: An upper limit of 1200°C is given as realistic for magmas derived from mantle related sources beneath continental margins. For model calculations we assume that no crystallisation occurs during the first stage. Therefore, the andesite minimum temperature is given by its liquidus temperature  $T_1^m$ , which is set at 1175°C in the model.

Table 2  
Lithospheric structure and rock properties used in the model

Structure unit	Depth interval(km) <sup>c</sup>	$A(\mu\text{W}/\text{m}^3)$	$\lambda(\text{W}/\text{mK})^a$	Density(g/cm <sup>3</sup> )
Upper crust	0–22	0.60	2.50	2.75 <sup>e</sup>
Lower crust	22–60	0.45 <sup>b</sup>	2.47 <sup>c</sup>	2.83 <sup>e</sup>
Lithospheric mantle	60–80	0.008	3.40	3.24 <sup>e</sup>
Melt <sup>d</sup>		0.008	4.00	2.80
Conduit, 20% melt	0–22	0.48	2.70	2.76
Conduit, 20% melt	22–60	0.36	2.60	2.82
Conduit, 20% melt	60–80	0.008	3.51	3.15

<sup>a</sup> Values at  $T = 0^\circ\text{C}$ .

<sup>b</sup> Pollack and Chapman (1977).

<sup>c</sup> Arndt et al. (1995): harmonic mean of gabbro (2.65), pyroxene–gneiss (2.64), and amphibolite (2.19),  $\lambda = 2.40 \text{ W m}^{-1} \text{ K}^{-1}$  and  $\lambda = 2.35 \text{ W m}^{-1} \text{ K}^{-1}$  if proportions are assumed to be 1:1:2 and 1:1:3, respectively.

<sup>d</sup> Basaltic melt, Singer et al. (1989).

<sup>e</sup> Omarini and Götze (1991) and Wigger et al. (1994).

The amount of heat released due to cooling of the andesite by 25°C leads to a slight increase of the country rock temperature in the conduit and a small degree of partial melting is triggered.

In order to test if mafic magmas are buoyantly stopped during ascent, we estimate the resulting conduit temperature  $T$  at a given depth by numerically solving the following energy balance equation:

$$Q - Q_r = \Phi c^m \rho^m T_1^m + (1 - \Phi) c^r \rho^r T, \quad (11)$$

with

$$Q = \Phi c^m \rho^m T^m + (1 - \Phi) c^r \rho^r T^r,$$

$$Q_r = (1 - \Phi) \rho^r X^r L^r,$$

where  $\Phi$  indicates the initial volume fraction of mafic melt within the conduit,  $c^m$  and  $c^r$  are the heat capacities of andesitic melt and wall rock and  $\rho^m$  and  $\rho^r$  denote the densities of melt and rock, respectively. The left hand-side of Eq. (11) is the conduit heat content at  $T^r$ ,  $Q$  is the initial heat content within the conduit without latent heat of wall rock fusion. In the case of wall rock fusion, the term  $Q_r$  takes into account the latent heat consumed by this process.

As reasoned in Section 3.1, we assume for computation that the mafic melt fraction within the con-

duit zone increases up to a level of 20% ( $\Phi = 0.2$ ). Fig. 5 shows the distribution of the melting degree  $X^r$  within the conduit after andesite cools to liquidus temperature as a function of depth and  $C_0^r$  for the parameter combination  $s^m = 0.2$  and  $s^s = 0.8$ . The assumption of  $C_0^r = 3.0$  wt% (Section 2.1.1) is an upper limit. However, the formation of magma will buffer the temperature at the site of its generation. For a granitic lithology, the temperature then lies between 750°C and 850°C, too low for the formation of large volumes of melt at dry conditions. Litvinovsky and Podladchikov (1993) therefore consider the introduction of additional water (or other volatiles) into the source region of the melt. Fig. 5 shows that values of  $C_0^r < 2.5$  are not sufficient to ensure the development of a PMZ density barrier with  $X^r \geq 0.17$  for subsequent andesite magmas. The critical PMZ at  $C_0^r = 3.0$  reaches down to the model Moho at 60 km depth. Thus, the model stops further andesite magma input at the Moho.

**Stage 3, stop of mafic melt ascent:** A critical melt fraction is reached at the end of stage 2 (i.e. the PMZ bulk density equals the andesite melt density), and the PMZ acts as a density barrier for subsequent mantle-derived magmas. The andesitic ascent above PMZ stops since there is no supply from below. This

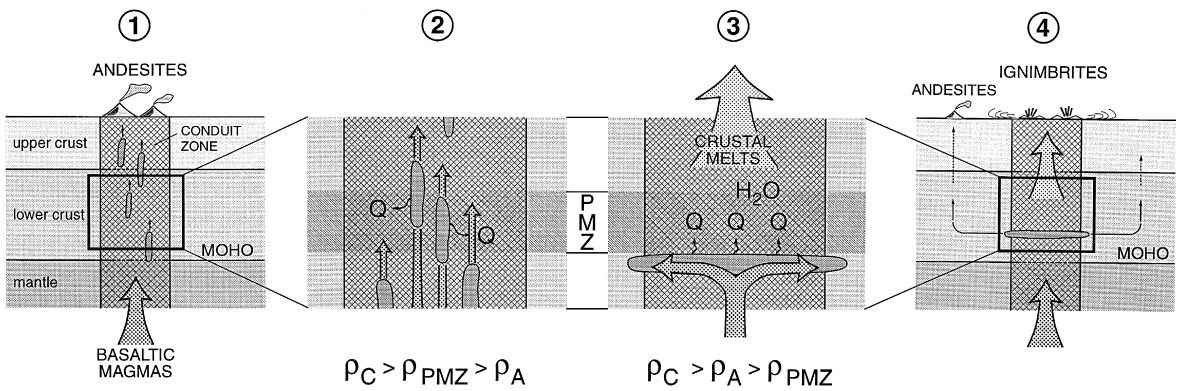


Fig. 4. 4-stage model to explain the onset of felsic magmatism as a consequence of an abating period of mafic magmatism: (1) Ongoing magma input from mantle through the crust results in mafic (andesitic) volcanism, focused in a conduit zone under the active arc. Change in subduction geometry (e.g. faster spreading rate, as mentioned by Pardo-Casas and Molnar (1987) for the central Andes in the Oligocene) leads to a greater magma input into the crust. (2) The magma input reaches its maximum. The increased ascent rate of andesitic melt causes an increased heat ( $Q$ ) input into the country rock. Due to temperature rise, a partial melt zone (PMZ) forms. (3) The PMZ acts as a density barrier when a critical melt fraction is reached, where the andesite density  $\rho_A$  is  $\geq \rho_{PMZ}$ . Subsequent melts pond below the PMZ. Due to this underplating, the andesite ascent above PMZ stops, partially freezes, and releases heat and water. Consequent crustal melting within and above the PMZ increases to a level which enables large-scale melt segregation. (4) Silicic ignimbritic volcanism takes place; at the same time, minor centres of andesite positioned beside the conduit zone are a consequence of basic magma volumes laterally deviated by the PMZ barrier.

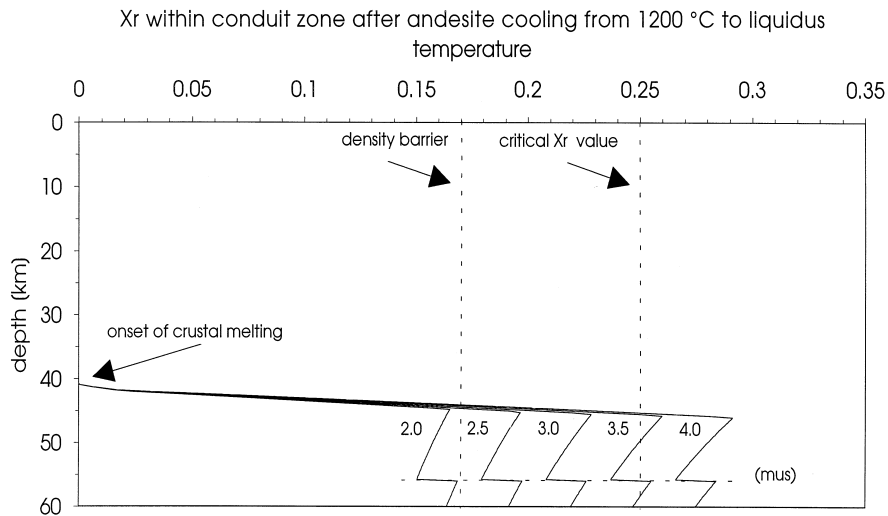


Fig. 5. Dependency of  $X^r$  within the conduit on depth on various initial crustal water contents  $C_0^r$  (2.0–4.0 wt%, as indicated by numbers) during stage 2. The andesite melt is cooled from 1200°C down to its model liquidus temperature of 1175°C. At surface, this temperature decrease is on the order of magnitude expected for cooling due to adiabatic decompression (0.3°C/km). Until  $\approx 41$  km depth no wall rock melting occurs. At depths greater than  $\approx 45$  km, the country rock is partially molten at degrees higher than 0.17 for  $C_0^r \geq 2.5$  wt%. The region indicated by a  $X^r \geq 0.17$  may act as a density barrier for subsequent andesite magmas. The change from  $F$  to  $f$  dominated melting is clearly marked at the first sharp change of  $X^r$ . The increase of  $X^r$  at around 55 km depth is due to the additional water released by the muscovite decomposition reaction (mus).

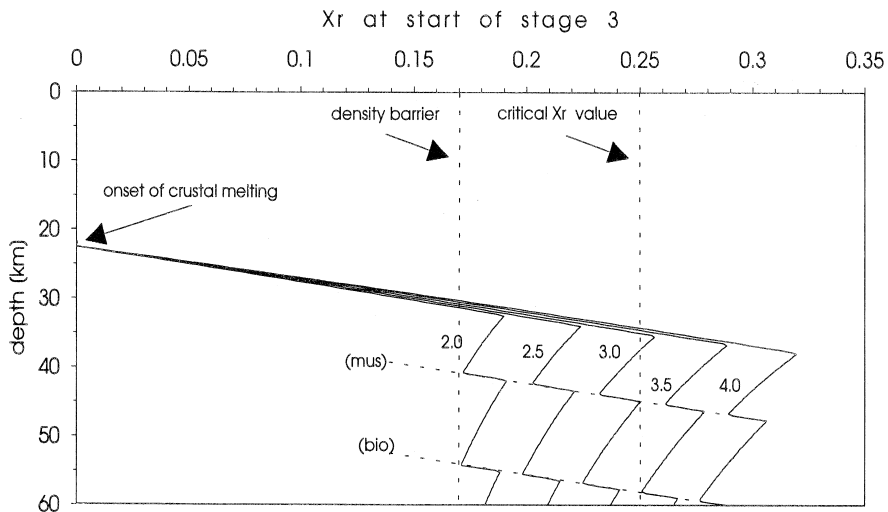


Fig. 6. Dependency of  $X^r$  within the conduit zone on depth at the start of stage 3 at various initial crustal water contents  $C_0^r$  (2.0–4.0 wt%, as indicated by numbers). In contrast to the results given in Fig. 5, the country rock and the andesitic melt are thermally equilibrated. Therefore, the onset of crustal melting is shifted from around 41 km up to around 23 km depth. The average temperature in the conduit zone falls below the andesite liquidus temperature. Thus, the latent heat  $L^m$  released by the andesitic melt becomes important. The sharp increases of  $X^r$  at around 40 and 55 km depth are due to the additional water released by muscovite and biotite decomposition reactions (mus, bio). At  $C_0^r \geq 3.0$  wt%, the critical threshold value of  $X^r$  of 0.25 for melt segregation is exceeded. As the calculated  $X^r$  indicate maximum values, a  $C_0^r \geq 3.0$  wt% must be supposed in the model.

is the initial stage for our simulations. Retained and stored within the crust, the andesite magma freezes and releases heat and water into the environment. The consequent melting within and above the PMZ increases to a level which enables large-scale melt segregation.

After development of a density barrier for subsequent mantle-derived magmas, we assume an instantaneous heat equilibration between intracrustal andesite which is stuck within the conduit, and country rock.

In this case, andesite melt freezing occurs and Eq. (11) is changed to:

$$Q - Q_r + \underbrace{\Phi \rho^m (1 - X^m) L^m}_{Q_{xx}} = [\Phi c_p^m \rho^m + (1 - \Phi) c_p^r \rho^r] T, \quad (12)$$

where the term  $Q_{xx}$  takes into account the latent heat contributed by andesite crystallisation.

Fig. 6 shows the  $X^r$ -depth distribution after thermal equilibration between andesite melt and wall rock for the same parameter combination as in Fig. 5.

**Stage 4, silicic volcanism:** Crustal-derived (ignimbritic) volcanism takes place; minor centres of andesite positioned beside the conduit are a consequence of mafic magma laterally deviated by the

PMZ barrier. The dominant melt composition within the conduit changes from mafic to felsic.

The total volume  $V$  of silicic melt generated in zones characterized by a particular  $X^r$  (e.g.  $X^r \geq 0.25$ ) is estimated by numerical computation of the integral:

$$V = \int_{X^r \geq 0.25} X^r dA \quad (13)$$

in the cross-section which gives the volume of potentially segregable magma per length of trench.

Two realistic cases of water saturation degrees in the mafic melt are focused on  $s^m = 0.2$  and  $s^m = 0.4$ . The degree of water saturation  $s^s$  for the felsic melt is varied between 0.8 and 1.0 by increments of 0.05. Such high degrees of water saturation are reasonable for the conditions at the moment of melt generation. After consumption of the available water, a further temperature increase causes the water-saturated solidus to be exceeded, leading to the formation of a water-undersaturated melt. Only this undersaturated melt is able to ascend to shallow depths or the surface without freezing (e.g. Johannes and Holtz, 1990, 1991).

The water amounts  $C^m$  and  $C^s$  calculated from Eqs. (3) and (4) as a function of pressure and

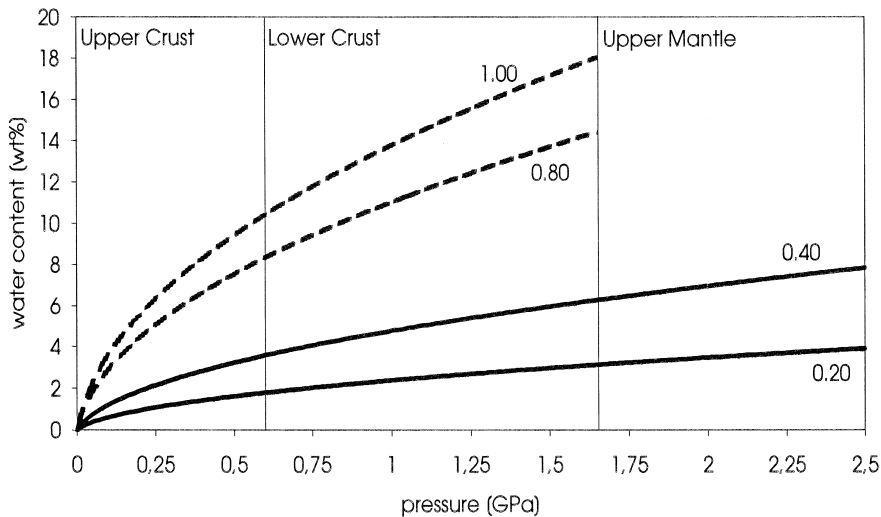


Fig. 7. Amount of water released by the andesitic melt ( $C^m$ ) at  $s^m = 0.2$  and  $s^m = 0.4$  as a function of pressure (solid lines). Amount of water dissolved by a silicic melt ( $C^s$ ) with saturation degrees  $s^s = 1.0$  and  $s^s = 0.8$  as a function of pressure (dotted lines). All curves calculated using Eqs. (3) and (4).

saturation level are shown in Fig. 7. Within the lower crust, the water content of a basic–intermediate magma can contribute roughly 10–50% of the total water amount required by a silicic melt, and will promote high degree of melting at low temperatures. Because hornblende is common in the phenocryst assemblage of Miocene to Recent central Andean andesites (Hahne et al., 1995), the water

content of the melts must have been sufficient for amphibole to be stable. Under middle to lower crust conditions the water content in the coexisting melt must have been  $\geq 3$  wt% (e.g. Eggler, 1972; Romick et al., 1992).

The time-dependent temperature development starting with the temperature field computed from Eq. (12) is simulated using Eq. (7).

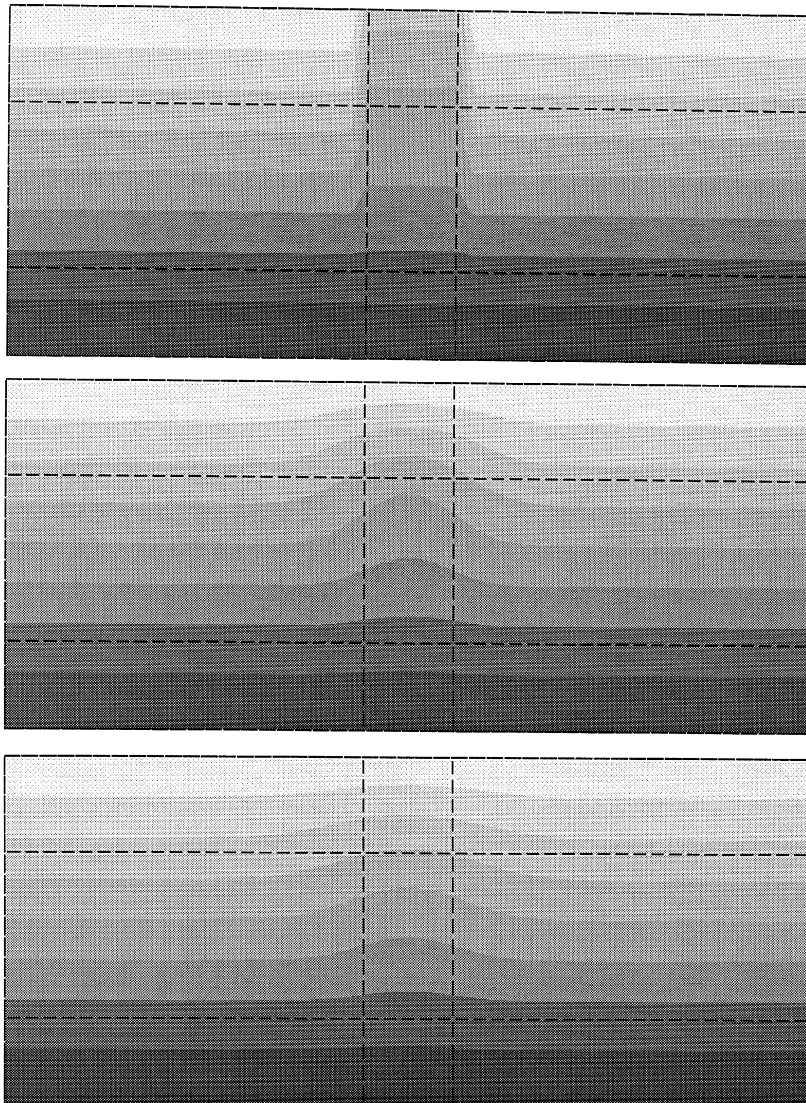


Fig. 8. Temperature distribution at initial time (upper panel) and after a cooling period of 2.5 (middle panel) and 5.0 Ma (lower panel). These results correspond to the cases  $s^m = 0.2$  and  $s^s = 0.8$ . Colours are incremented by steps of 150°C. Light grey: 0–150°C; black: 1050–1200°C. The black dashed lines indicate the model areas as defined in Fig. 3.

Fig. 8 shows the temperature fields after a cooling period of 0.0, 2.5 and 5.0 Ma; the related spatial distributions of melt clusters at different degree of partial melting within the crust are shown in Fig. 9. As expected from the model, the zones with highest degrees of melting are located within the conduit zone borders as a result of the additional water release from the mafic melt. The occurrence of

molten zones with  $X^f \geq 0.2$  outside of the conduit is restricted to depths exceeding 39 km. This is in accordance with the concept of a migmatitic lower crust. It is remarkable that the main vertical focus of the  $X^f \geq 0.20$  area is located within the depth range of a standard crustal thickness.

The volumes of crustal melts in zones indicated by  $X^f \geq 0.15$  are calculated using Eq. (13) for differ-

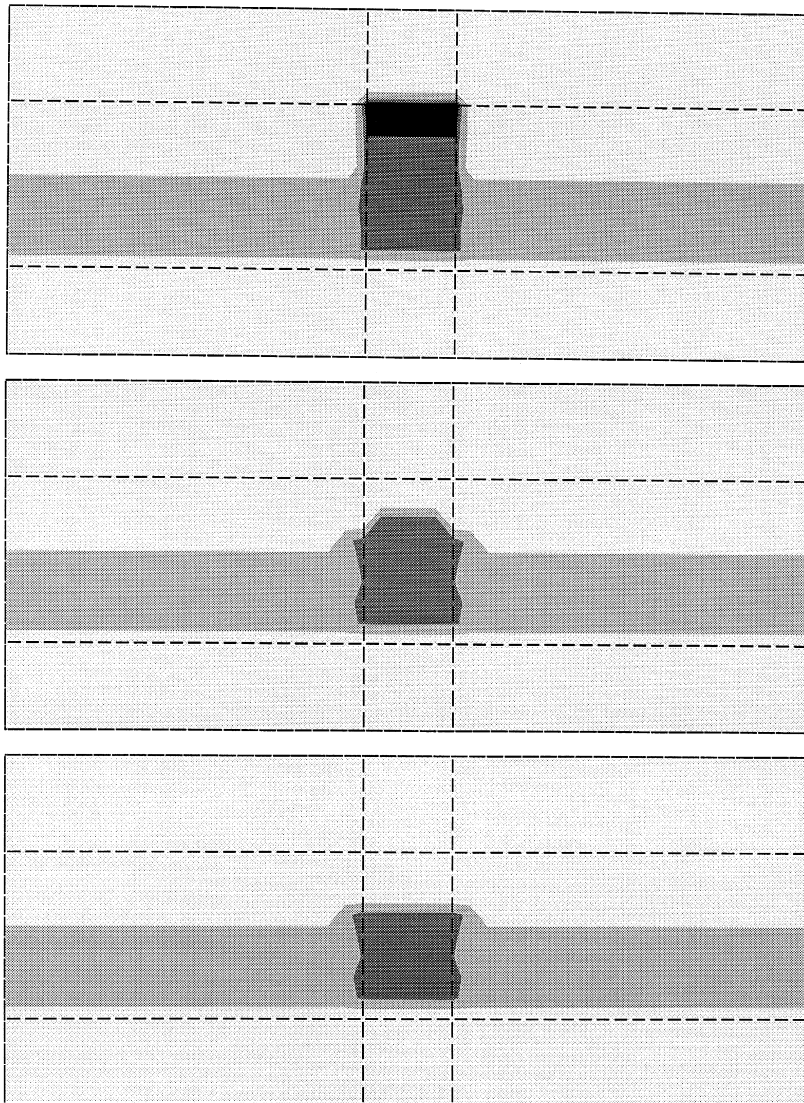


Fig. 9. Spatial distribution of melt clusters of different degree of partial melting within the crust based on the temperature fields given in Fig. 8. Light grey:  $X^f < 0.10$ ; grey:  $X^f \geq 0.10$ ; dark grey:  $X^f \geq 0.20$ ; and black:  $X^f \geq 0.25$ . These results correspond to the cases  $s^m = 0.2$  and  $s^s = 0.8$ .

ent times of conduit cooling. Two cases of andesite water saturation are taken into consideration,  $s^m = 0.2$  and  $s^m = 0.4$ . Fig. 10 shows the calculated cumulative melt volumes per km arc in dependence of melting degree and model time. The maximum values of  $X^f$  vary between 0.31 ( $s^m = 0.2$ ) and 0.36 ( $s^m = 0.4$ ) and are reached after 2.5 Ma.

In both cases, remarkable melt volumes of 210–270 km<sup>3</sup>/km arc, indicated by  $X^f \geq 0.25$ , are formed. Higher crustal water content at  $s^m = 0.4$  results in the formation of zones with increased  $X^f$ .

Only a small percentage of the original magma chamber volume is emptied by ignimbritic eruption. Smith (1979) estimated that not more than 10 vol% of the chamber volume is removed by any one pyroclastic eruption. However, Crisp (1984) estimated a ratio of intrusive to extrusive volumes of  $\approx 6:1$  from scarce data for the central Andes. If the Crisp (1984) constraint is taken into account, from our calculated  $\approx 250$  km<sup>3</sup>/km arc approximately 36 km<sup>3</sup>/km arc could erupt.

DeSilva (1989b) gives estimates of volumes of erupted ignimbrite in the central Andean volcanic zone (CVZ). The volume of individual ignimbrites vary from 100 km<sup>3</sup> to more than 1000 km<sup>3</sup>. In total,

DeSilva (1989b) approximated a volume of  $10^4$  km<sup>3</sup> magma over a period of 9 Ma in the 21°30'–23°30'S portion of the CVZ. Francis and Hawkesworth (1994) estimated a similar value of  $1.5 \times 10^4$  km<sup>3</sup> silicic pyroclastic rocks within CVZ. The 21°30'–23°30'S portion covers a length of  $\approx 225$  km. We assume the ignimbrite volume to be dense rock equivalent and take this as an upper estimate of the magma volume. Thus, assuming a homogeneous distribution of melt sources,  $\approx 40$  km<sup>3</sup>/km arc of segregable melt in the source region are required to provide 10,000 km<sup>3</sup>. From our calculations of roughly 250 km<sup>3</sup> segregable melt per km arc, an intrusive to extrusive ratio of around 5.25:1 would reproduce the observations. However, it must be considered that the assumed ignimbrite volume is an overestimate. Therefore, our calculated intrusive to extrusive ratios are lower limits.

Once formed, felsic magmas can be transported within dikes through the continental crust at ascent rates of  $\approx 10^{-2}$  ms<sup>-1</sup> (Petford et al., 1993; Petford, 1996). Thus, large plutons or shallow magma chambers can be filled in less than  $10^4$  a. Compared to the time required for melt formation, the time lag of magma ascent is negligible.

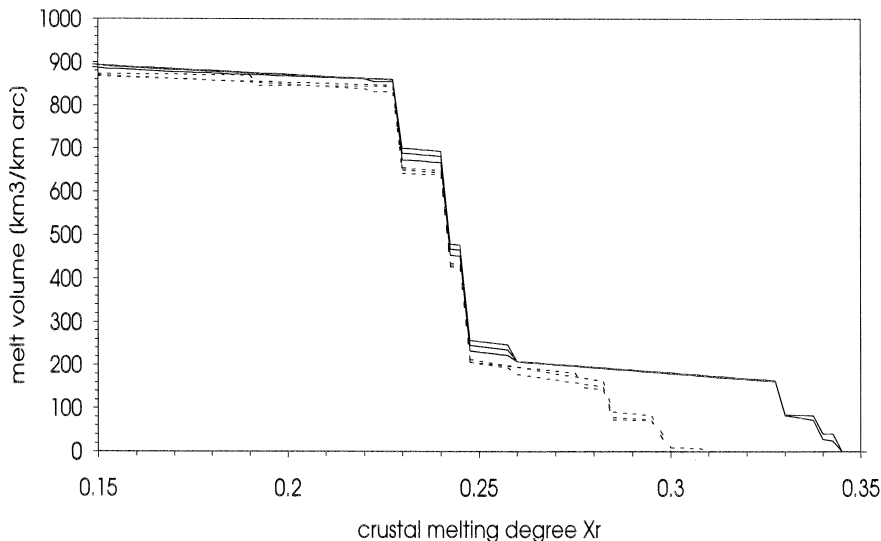


Fig. 10. Calculated cumulative crustal melt volumes (summed over the entire cross section) vs. melting degree  $X^f$ . For a particular  $X^f$ , the melt volume represents the sum of zones molten up to a degree higher or equal to this  $X^f$ . Dotted lines are estimated with  $s^m = 0.2$ ; the solid lines show the results of the assumption of  $s^m = 0.4$ .

#### 4. Conclusions

At active continental margins, the input of mafic magma into the crust is controlled by a variety of parameters. A change in the subduction geometry or spreading rate may have a dramatic influence on the mafic melt generation and ascent behaviour, and thus on the crustal temperature field.

Our results indicate that crystallisation of mafic melts within their crustal conduits can influence the spatial and volumetric extent of wall rock melting by heat loss and water release.

Within some millions of years, large melt volumes are formed. From these, only those fractions are able to escape which are generated in regions where the critical melting degree for segregation is exceeded. This threshold melting degree depends on a variety of parameters which are often unknown. We have estimated the melt volumes in the range of potential critical melting degrees between 0.15 and 0.35. These estimated melt volumes either ascent to shallower crustal levels or to the surface, and some may just act as contaminants for mafic magmas. In the example of the central Andes, we calculated from rough data and under the consideration of a critical melt fraction 25% (Thompson and Connolly, 1995; Vigneresse et al., 1996) segregable melt volumes, high enough to explain intrusive/extrusive ratios up to 5.25:1. In the case of the ‘low melt fraction window’ proposed by Barboza and Bergantz (1996) this ratio increases up to 21.5:1.

The proposed model can explain the observed time-dependent change of the dominant magmatic expression at surface from basic-intermediate to intermediate-acidic composition.

#### Acknowledgements

The authors gratefully acknowledge S. DeSilva, Indiana State University, USA for fruitful discussion and providing his ideas to the ignimbrite genesis in the central Andes as valuable input to our model. D. Sahagian, A. Proussevitch, G.W. Bergantz and an anonymous reviewer provided very helpful and constructive reviews, which improved an earlier version of the manuscript. We thank R. Trumbull, Geo-ForschungsZentrum (GFZ), Potsdam, for discussions

and valuable comments on the manuscript. This work was done in cooperation with the SFB-267 collaborative research programme, ‘Deformation in the Andes’, in Berlin and Potsdam.

#### Appendix A. Mineral reactions taken into account for model calculation

(1) Water saturated solidus for granitic rocks (Whitney, 1988; Philpotts, 1990); values  $p(x)$  for given points  $x_i$ ,  $i = 1, \dots, 7$ , used for linear interpolation

$T$ (°C)	935	800	740	680	660	640	600
$p$ (GPa)	0	0.05	0.1	0.2	0.3	0.4	1.35

(2) Melting curves for water-undersaturated conditions based on decomposition reactions of water-bearing mineral phases (Whitney, 1988; Philpotts, 1990). The minimum pressure–temperature combination is given by the wet solidus curve (see above), where,  $T$  (°C) and  $p$  (GPa):

- muscovite (out):  
 $\text{musc} + \text{qz} + \text{Na-fsp} \leftrightarrow \text{sill} + \text{K-fsp} + \text{melt}$   
 $T = 139p + 624.4;$
- biotite (out):  
 $\text{bio} + \text{qz} + \text{Na-fsp} \leftrightarrow \text{K-fsp} + \text{pyx} + \text{melt}$   
 $T = 126p + 739.5;$
- hornblende (out):  
 $\text{hbl} + \text{qz} + \text{fsp} \leftrightarrow \text{pyx} + \text{melt}$   
 $T = 105p + 898.0.$

#### References

- Arndt, J., Partzsch, G.M., Schilling, F., 1995. Petrophysikalische Eigenschaften von Mineralien und Gesteinen der andinen Unterkruste in Abhängigkeit von Druck und Temperatur. In: Deformation processes in the central Andes. Collaborative Research Programme 267, 1993–1995, Free University Berlin.
- Arzi, A.A., 1978. Critical phenomena in the rheology of partially melted rock. *Tectonophysics* 44, 173–184.
- Asmerom, Y., Patchett, P.J., Damon, P.E., 1991. Crust–mantle interaction in continental arcs: Inferences from Mesozoic arc in southwestern United States. *Contrib. Mineral. Petrol.* 107, 124–134.
- Barboza, S.A., Bergantz, G., 1996. Dynamic model of dehydration melting motivated by a natural analogue: Applications to the Ivrea–Verbano zone, northern Italy. *Trans. R. Soc. Edinburgh Earth Sci.* 87, 23–31.
- Bergantz, G.W., 1989. Underplating and partial melting: Implica-

- tions for melt generation and extraction. *Science* 245, 1093–1095.
- Bergantz, G.W., Dawes, R., 1994. Aspects of magma generation and ascent in continental lithosphere. In: Ryan, M. (Ed.), *Magmatic Systems*. Academic Press, pp. 291–317.
- Burnham, C.W., 1975. Water and magmas. A mixing model. *Geochim. Cosmochim. Acta* 39, 1077–1084.
- Coira, B., Kay, S.M., Viramonte, J., 1993. Upper Cenozoic magmatic evolution of the Argentine Puna: A model for changing subduction geometry. *Int. Geol. Rev.* 35, 677–720.
- Crisp, J., 1984. Rates of magma emplacement and volcanic output. *J. Volcanol. Geotherm. Res.* 20, 177–211.
- DeSilva, S.L., 1989a. Altiplano-Puna volcanic complex of the central Andes. *Geology* 17, 1102–1106.
- DeSilva, S.L., 1989b. Geochronology and stratigraphy of the ignimbrites from the 21°30'S to 23°30'S portion of the central Andes of northern Chile. *J. Volcanol. Geotherm. Res.* 37, 93–131.
- Dvorkin, J., Nur, A., Mavko, G., Ben-Avraham, Z., 1993. Narrow subducting slabs and the origin of backarc basins. *Tectonophysics* 227, 63–79.
- Eggler, D.H., 1972. Amphibole stability in H<sub>2</sub>O undersaturated calc-alkaline melts. *Earth Planet. Sci. Lett.* 15, 28–34.
- Francis, P.W., Hawkesworth, C.J., 1994. Late Cenozoic rates of magmatic activity in the central Andes and their relationship to continental crust formation and thickening. *J. Geol. Soc. London* 151, 845–954.
- Graham, I.J., Cole, J.W., Briggs, R.M., Gamble, J.A., Smith, I.E.M., 1995. Petrology and petrogenesis of volcanic rocks from the Taupo volcanic zone: A review. *J. Volcanol. Geotherm. Res.* 68, 59–87.
- Grove, T.L., Kinzler, R.J., Baker, M.B., Donnelly-Nolan, J.M., Leshner, C.E., 1988. Assimilation of granite by basaltic magma at burnt lava flow, Medicine Lake volcano, northern California: Decoupling of heat and mass transfer. *Contrib. Mineral. Petrol.* 99, 320–343.
- Hahne, K., Wittenbrink, R., Emmermann, R., Büsch, W., Trumbull, R., 1995. Magmenbildung und Krustengeneese: Neogene Vulkanite der Zentralen Vulkanzone, nord Chile. In: *Deformation Processes in the Central Andes. Collaborative Research Programme* 267, 1993–1995, Free University Berlin.
- Hildreth, W., Moorbath, S., 1988. Crustal contributions to arc magmatism in the Andes of central Chile. *Contrib. Mineral. Petrol.* 98, 455–489.
- Hochstein, M.P., 1995. Crustal heat transfer in the Taupo volcanic zone (New Zealand). Comparison with other volcanic arcs and explanatory heat source models. *J. Volcanol. Geotherm. Res.* 68, 117–151.
- Holdaway, M.J., 1971. Stability of andalusite and the aluminium silicate phase diagram. *Am. J. Sci.* 271, 97–131.
- Holtz, F., Behrens, H., Dingwell, D.B., Johannes, W., 1995. H<sub>2</sub>O solubility in haplogranitic melts: Compositional, pressure and temperature dependence. *Am. Mineral.* 80, 94–108.
- Huppert, H.E., Sparks, R.S.J., 1988a. The generation of granitic magmas by intrusion of basalt into continental crust. *J. Petrol.* 29, 599–624.
- Huppert, H.E., Sparks, R.S.J., 1988b. The fluid dynamics of crustal melting by injection of basaltic sills. *Trans. R. Soc. Edinburgh Earth Sci.* 79, 237–243.
- Hyndman, D.W., 1981. Controls on source and depth of emplacement of granitic magmas. *Geology* 9, 244–249.
- Johannes, W., Holtz, F., 1990. Formation and composition of H<sub>2</sub>O-undersaturated granitic melts. In: Ashworth, J.R., Brown, M. (Eds.), *High Temperature Metamorphism and Crustal Anatexis*. Unwin Hyman Ltd.
- Johannes, W., Holtz, F., 1991. Formation and ascent of granitic magmas. *Geol. Rundsch.* 80 (2), 225–231.
- Marsh, B.D., 1989. Magma Chambers. In: Wetherhill, G.W. et al. (Eds.), *Annu. Rev. Earth Planet. Sci.* 17, 439–474.
- Mysen, B.O., 1977. The solubility of H<sub>2</sub>O and CO<sub>2</sub> under predicted magma genesis conditions and some petrological and geophysical implications. *Rev. Geophys. Space Phys.* 15, 351–361.
- Leeman, W.P., 1983. The influences of crustal structure on compositions of subduction-related magmas. *J. Volcanol. Geotherm. Res.* 18, 561–588.
- Litvinovsky, B.A., Podladchikov, Yu.Yu., 1993. Crustal anatexis during influx of mantle volatiles. *Lithos* 30, 93–107.
- Omarini, R.H., Götze, H.J. (Eds.), 1991. *Global Geoscience Transect 6. Central Andean Transect, Nazca Plate to Chaco Plains southwestern Pacific ocean, northern Chile and northern Argentina*. American Geophysical Union, Publication No. 192 of the International Lithosphere Program.
- Pardo-Casas, F., Molnar, P., 1987. Relative motion of the Nazca (Farallon) and South American plates since Late Cretaceous time. *Tectonics* 6, 233–248.
- Patchett, P.J., 1980. Thermal effects of basalt on continental crust and crustal contamination of magmas. *Nature* 283, 559–561.
- Peacock, S.M., 1993. Large-scale hydration of the lithosphere above subducting slabs. *Chem. Geol.* 108, 49–59.
- Petford, N., Kerr, R.C., Lister, J.R., 1993. Dike transport of granitoid magmas. *Geology* 21, 845–848.
- Petford, N., 1996. Dykes or diapirs?. *Trans. R. Soc. Edinburgh Earth Sci.* 87, 105–114.
- Philpotts, A.R., 1990. *Principles of Igneous and Metamorphic Petrology*. Prentice Hall, New Jersey.
- Pollack, H.N., Chapman, D.S., 1977. On the regional variation of heat flow, geotherm and lithospheric thickness. *Tectonophysics* 38, 279–296.
- Rivers, M.L., Carmichael, I.S.E., 1987. Ultrasonic studies of silicate melts. *J. Geophys. Res.* 92 (B7), 9247–9270.
- Romick, J.D., Kay, S.M., Kay, R.W., 1992. The influence of amphibole fractionation on the evolution of calc-alkaline andesite and dacite tephra from the central Aleutians, Alaska. *Contrib. Mineral. Petrol.* 112, 101–118.
- Sandiford, M., Powell, R., 1990. Some isostatic and thermal consequences of the vertical strain geometry in convergent orogens. *Earth Planet. Sci. Lett.* 98, 154–165.
- Schatz, J.F., Simmons, G., 1972. Thermal conductivity of earth materials at high temperatures. *J. Geophys. Res.* 77, 6966–6983.
- Schilling, F.R., Brasse, H., Partzsch, G.M., Schmitz, M., 1995. Evidence for partial melt in the western Cordillera in the central Andes. *Ann. Geophys.* 14 (Suppl. 1), C187.

- Schmitt-Riegraf, C., Pichler, H., 1988. Cenozoic ignimbrites of the central Andes; a new genetic model. In: Bahlburg, H., Bretkreuz, C., Giese, P. (Eds.), *The Southern Central Andes. Lecture Notes in Earth Sciences* 17, Springer Verlag, Heidelberg, Berlin, pp. 183–197.
- Schmitz, M., 1994. A balanced model of the southern central Andes. *Tectonics* 13, 484–492.
- Schwarz, G., 1995. Elektisch hochleitfähige Zonen in den südlichen zentralen Anden: Abbilder tektonischer Prozesse? In: *Deformation Processes in the Central Andes. Collaborative Research Programme* 267, 1993–1995, Free University Berlin.
- Schwarz, G., Chong Dias, G., Krüger, D., Martinez, E., Massow, W., Rath, V., Viramonte, J., 1994. Crustal high conductivity zones in the Southern Andes. In: Reutter, K.J., Scheuber, E., Wigger, P.J. (Eds.), *Tectonics of the Southern Central Andes*. Springer Verlag, Berlin, 333 pp.
- Singer, B.S., Myers, J.D., Linnemann, S.R., Angevine, C.L., 1989. The thermal history of ascending magma diapirs and the thermal and physical evolution of magmatic conduits. *J. Volcanol. Geotherm. Res.* 37, 273–289.
- Smith, R.L., 1979. Ash-flow magmatism. *Geol. Soc. Am. Spec. Pap.* 180, 5–27.
- Tepper, J.H., Nelson, B.K., Bergantz, G.W., Irving, A.J., 1993. Petrology of the Chilliwack batholith, North Cascades, Washington: Generation of calc-alkaline granitoids by melting of mafic lower crust with variable water fugacity. *Contrib. Mineral. Petrol.* 113, 333–351.
- Thompson, A.B., Connolly, A.D., 1995. Melting of the continental crust: Some thermal and petrological constraints on anatexis in continental collision zones and other tectonic settings. *J. Geophys. Res.* 100, 15565–15579.
- Touloukian, Y.S., Judd, W.R., Roy, R.F. (Eds.), 1989. *Physical properties of rocks and minerals. CINDAS Data Series on Material Properties*, vol. II-2. Hemisphere Publishing Corp.
- Tovish, A., Schubert, G., Luyendyk, B.P., 1978. Mantle flow and the angle of subduction: Non-Newtonian corner flows. *J. Geophys. Res.* 83, 5892–5898.
- Turcotte, D.L., Schubert, G., 1982. *Geodynamics: Application of Continuum Physics to Geological Problems*. John Wiley and Sons, New York, 450 pp.
- Van der Molen, I., Paterson, M.S., 1979. Experimental deformation of partially-melted granite. *Contrib. Mineral. Petrol.* 70, 299–318.
- Vignerresse, J.L., Barbey, P., Cuney, M., 1996. Rheological transitions during partial melting and crystallisation with application to felsic magma segregation and transfer. *J. Petrol.* 37, 1579–1600.
- Von Bargen, N., Waff, H.S., 1986. Permeabilities, interfacial areas and curvatures of partially molten systems: results of numerical computations of equilibrium microstructures. *J. Geophys. Res.* 91, 9261–9276.
- Whitney, J.A., 1988. The origin of granite: The role and source of water in the evolution of granitic magmas. *Geol. Soc. Am. Bull.* 100, 1889–1897.
- Wickham, S.C., 1987. The segregation and emplacement of granitic magmas. *J. Geol. Soc. London* 144, 281–297.
- Wigger, P., Schmitz, M., Araneda, M., Asch, G., Baldzuhn, S., Giese, P., Heinsohn, W.-D., Matrinez, E., Ricaldi, E., Röwer, P., Viramonte, J., 1994. Variation in the crustal structure of the Southern central Andes deduced from seismic refraction investigation. In: Reutter, K.J., Scheuber, E., Wigger, P.J. (Eds.), *Tectonics of the Southern Central Andes*. Springer Verlag, Berlin, 333 pp.
- Wilson, M., 1991. *Igneous Petrogenesis*. 2nd ed. Harper Collins Academic, London.
- Wyllie, P.J., 1984. Constraints imposed by experimental petrology on possible and impossible magma sources and products. *Philos. Trans. R. Soc. London A* 310, 439–456.
- Zen, E.A., 1988. Thermal modelling of step-wise anatexis in a thrust thickened sialic crust. *Trans. R. Soc. Edinburgh Earth Sci.* 79, 223–235.
- Zen, E.A., 1992. Using granite to image the thermal state of the source terrane. *Trans. R. Soc. Edinburgh Earth Sci.* 83, 107–114.